Eur. Phys. J. B **42**, 467–475 (2004)
DOI: 10.1140/epjb/e2005-00004-0

THE EUROPEAN PHYSICAL JOURNAL B

Dynamics of self-localized excitations in a polyacene chain

Z. An[1,2,a] and C.Q. Wu[2]

[1] College of Physics, Hebei Normal University, 050016 Shijiazhuang, China
[2] Department of Physics, Fudan University, 200433 Shanghai, China

Received 3 September 2004
Published online 18 January 2005 –

Abstract. Dynamical formation processes of self-localized excitations induced by charge injection or photoexcitations in a polyacene chain are investigated by a nonadiabatic dynamic method. The polyacene chain is treated as two alternatively coupled polyacetylene chains. The initial lattice configuration is taken as the pristine polyacene chain. It contains an interchain-coupled neutral soliton as a consequence of odd-number sites in each of the two chains. The nonadiabatic dynamical processes are carefully investigated in the following physical cases: (1) electron injection; (2) electron transition from the highest occupied molecular orbital (HOMO) to the lowest unoccupied molecular orbital (LUMO); (3) electron transition from HOMO to the localized soliton level, and (4) electron-hole pair excited at the continuum absorbtion edge for light polarized parallel to the chain. It is interestingly found that the centers of the electron and the hole excited by light polarized parallel to the chain are separated. Therefore, the photogenerated charge carriers should be favorable in polyacene, which is remarkably different from those found in a single polyacetylene chain.

PACS. 71.38.Ht Self-trapped or small polarons – 71.35.Aa Frenkel excitons and self-trapped excitons – 71.38.-k Polarons and electron-phonon interactions

1 Introduction

There have been considerable amounts of research works devoted to the study of nonlinear elementary excitations in conjugated polymers, such as soliton, polaron, and neutral polaron-exciton [1]. The motivation behind these works stems from the fact that these excitations play an important role in optoelectronic devices based on conjugated polymers, including field-effect transistors, light-emitting diodes, photocells and lasers[2–6]. For example, the charged polarons serve as charge carriers in these devices, and the luminescence originates from the polaron-exciton decay. Therefore, understanding the formation processes and characteristics of these excitations is fundamentally important to provide guidelines for improvement of the performance of these polymeric devices.

Polyacetylene, the simplest conjugated polymer, has been widely investigated as the prototype example [7]. Most of the theoretical works investigating self-trapping excitations in conjugated polymers have been focused on a single polyacetylene chain. In order to describe the bulk properties of polyacetylene, however, researchers have investigated the effect of interchain interactions between two polyacetylene chains, and found that even small interchain coupling can have a significant effect [8–10]. Polyacene, linearly fused aromatic rings, can be considered as two polyacetylene chains strongly coupled by cross alternate interactions, see Figure 1. Therefore, it is expected that elementary excitations in polyacene chain should be remarkably different from those in a single polyacetylene chain.

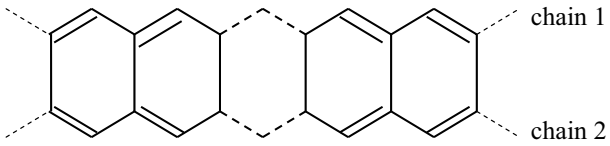

Fig. 1. The schematic representation of the structure of a pristine polyacene chain.

Indeed, as a novel conducting polymer, the electronic structure and elementary excitations of polyacene have long been the object of theoretical studies [11–23], though the long polyacene chain has not been synthesized yet. Earlier theoretical works [11–15] have devoted to the ground state of an infinite polyacene chain, with a controversial result on the bond alternation of the chain. While the nonalternant structure was suggested [11,12], many works indicated that the alternate bond structure with a corresponding gap about 0.4 eV is stable [13–15], Recently, the projector quantum Monte Carlo calculation and the density matrix renormalization group (DMRG) study considering electron-electron interactions have also confirmed that the bond alternated state is more favorable [16,17].

[a] e-mail: zan@fudan.edu.cn

Employing an extended Su-Schrieffer-Heeger (SSH) model [24], Sabra has studied the polaronic charge transfer between the two chains in polyacene, in the cases of polaron and bipolaron given initially in one chain [19]. Later, Li et al. investigated the effects of electron-electron interactions on the polaronic excitations with the SSH-Hubbard model [20,21]. Recently, we have investigated the optical absorptions and localized phonons due to these elementary excitations in a long but finite polyacene chain [22,23]. It has been indicated that polyacene possesses different absorbtion spectrum from that of a single polyacetylene chain. While all these works have concerned the static properties of these excitations in polyacene, their dynamic properties have not yet been studied so far.

In fact, the dynamic properties of these excitations in polymers, such as their formation dynamics, transport in an external field and so on, are believed to be of fundamental importance for polymeric devices, and are attracting more and more attentions. For example, the excitation dynamics properties in single polyacetylene chain have been investigated within an adiabatic dynamic method [25,26]. Recently, by using a nonadiabatic dynamic model, we have studied the polaron formation and its transportation in a metal/polymer/metal structure [27], and Stafström et al. have dealt with the polaron migration between two neighboring polyacetylene chains [28]. However, the excitation dynamics in polyacene remains to be investigated.

In this paper, by using a nonadiabatic dynamic method, we simulate dynamical formations of elementary excitations created through charge injection or photoexcitations in a long but finite polyacene chain, and investigate their physical features. The results are also compared with that of a single polyacetylene chain. The paper is organized as follows. In Section 2 we describe briefly the theoretical model and numerical method used in this work. In Section 3 the dynamic process of various excitations will be discussed. A summary is given in the last section.

2 Model and numerical method

The SSH model and its extended versions have achieved a great success in describing the electronic structure and bond distortion of conjugated polymers [24]. The Hamiltonian we consider in this paper is

$$H = H_{\rm SSH} + H_{int}, \tag{1}$$

where the first term is the standard SSH Hamiltonian describing the intrachain interactions in each chain,

$$H_{\rm SSH} = -\sum_{j,n,s}\left[t_0 - \alpha\left(u^x_{j,n+1} - u^x_{j,n}\right)\right]\left(c^+_{j,n+1,s}c_{j,n,s} + c^+_{j,n,s}c_{j,n+1,s}\right) + \frac{K}{2}\sum_{j,n}\left(u_{j,n+1} - u_{j,n}\right)^2 + \frac{M}{2}\sum_{j,n}\left(\dot{u}^x_{j,n}\right)^2, \tag{2}$$

where $j = 1, 2$ denotes the chain index, the site index n runs from 1 to $2m + 1$ for a polyacene chain which is composed of m aromatic rings, the quantity t_0 is the transfer integral of π-electrons in an undimerized lattice, α the electron-lattice coupling constant, $u^x_{j,n}$ is the lattice displacements of the nth site on chain j from its equidistant position along the chain direction. The operator $c^+_{j,n,s}(c_{j,n,s})$ creates (annihilates) a π-electron with spin s at the nth site on chain j. The second and the last terms in equation (2) represent the lattice elastic potential energy and kinetic energy, respectively. K is the elastic constant due to the σ bonds and M is the mass of a site. The second term in equation (1) describes the alternate interchain interactions,

$$H_{int} = -\sum_{n,s}\Big[\left(t_1 - (-1)^n t_2\right) - \frac{\alpha}{2}\left(1 - (-1)^n\right)\left(u^y_{1,n} - u^y_{2,n}\right)\Big]\left(c^+_{1,n,s}c_{2,n,s} + c^+_{2,n,s}c_{1,n,s}\right) + \frac{K}{2}{\sum_{n}}'\left(u^y_{1,n} - u^y_{2,n}\right)^2 + \frac{M}{2}\sum_{j,n}\left(\dot{u}^y_{j,n}\right)^2, \tag{3}$$

here t_1 and t_2 describe the alternate interchain interactions, $t_1 = t_2$ corresponds to the case of polyacene, $u^y_{j,n}$ is the lattice displacements of the nth site on chain j from its equidistant position vertical to the chain direction. Different from those used in previous works [19–23] where the bonds linking the two chains are fixed, we have also considered these bonds variable due to the electron-lattice interactions. The prime in equation (3) indicates the summation is only for the sites bonded between the two chains. Our results show that the localized distortions induced by charge injection or photoexcitation are also formed in these cross bonds as the same as those in chain direction, see Section 3.

The bond configuration and electronic structure of a pristine polyacene, which will be taken as the initial condition of the following dynamic simulations, can be obtained by minimizing the total static energy. For that, we can write down the following self-consistent equations of the bond configuration $\left\{u^x_{j,n}, u^y_{j,n}\right\}$ and the electronic wave functions $\{\phi_\mu(j,n)\}$ [29,30]:

$$\varepsilon_\mu\phi_\mu(j,n) = -\left[t_0 - \alpha\left(u^x_{j,n+1} - u^x_{j,n}\right)\right]\phi_\mu(j,n+1) - \left[t_0 - \alpha\left(u^x_{j,n} - u^x_{j,n-1}\right)\right]\phi_\mu(j,n-1) - \Big[\left(t_1 - (-1)^n t_2\right) - \frac{\alpha}{2}\left(1 - (-1)^n\right)\left(u^y_{1,n} - u^y_{2,n}\right)\Big]\phi_\mu(j',n), \quad (j' \neq j) \tag{4}$$

$$u^x_{j,n+1} - u^x_{j,n} = -\frac{2\alpha}{K}\left[\sum_{\mu}^{occ.}\phi_\mu(j,n)\,\phi_\mu(j,n+1) - \frac{1}{2m}\sum_{\mu,n}^{occ.}\phi_\mu(j,n)\,\phi_\mu(j,n+1)\right], \tag{5}$$

and

$$u^y_{1,n} - u^y_{2,n} = -\frac{2\alpha}{K}\left[\sum_{\mu}^{occ.}\phi_\mu(1,n)\,\phi_\mu(2,n) - \frac{1}{m+1}\sum_{\mu,n}^{occ.}\phi_\mu(1,n)\,\phi_\mu(2,n)\right], \quad (6)$$

where ε_μ is the eigenvalue of μth energy level. We have used the constraints $\sum_n \left(u^x_{j,n+1} - u^x_{j,n}\right) = 0$ and $\sum'_n \left(u^y_{1,n} - u^y_{2,n}\right) = 0$ to prevent the polymer chain from collapsing.

Once the initial lattice configuration $\{u_{j,n}\}$ and the electron distribution $\{\phi_\mu(j,n)\}$ are determined, the lattice configuration at any time $t(>0)$ can be obtained by the equation of motion for the atom displacements

$$M\,\ddot{u}^x_{j,n} = -K\left(2u^x_{j,n} - u^x_{j,n+1} - u^x_{j,n-1}\right) + 2\alpha\left[\rho_{jn,jn+1}(t) - \rho_{jn,jn-1}(t)\right], \quad (7)$$

and

$$M\,\ddot{u}^y_{j,n} = -K\left(u^y_{j,n} - u^y_{j',n}\right) + (-1)^j 2\alpha\rho_{jn,j'n}(t) \quad (8)$$

where the density matrix ρ is defined as

$$\rho_{jn,j'n'}(t) = \sum_k \Phi_{j,n,k}(t)\, f_k \Phi^*_{j',n',k}(t) \quad (9)$$

f_k is the time-independent distribution function and is determined by the initial condition, the electronic wave functions $\Phi_{j,n,k}(t)$ are the solution of the time-dependent Schrödinger equation

$$i\hbar\dot{\Phi}_{j,n,k}(t) = -\left[t_0 - \alpha\left(u^x_{j,n+1} - u^x_{j,n}\right)\right]\Phi_{j,n+1,k}(t) - \left[t_0 - \alpha\left(u^x_{j,n} - u^x_{j,n-1}\right)\right]\Phi_{j,n-1,k}(t) - \Big[(t_1 - (-1)^n t_2) - \frac{\alpha}{2}\left(1 - (-1)^n\right)\left(u^y_{1,n} - u^y_{2,n}\right)\Big]\Phi_{j',n,k}(t). \quad (j' \neq j). \quad (10)$$

The coupled differential equations (7), (8) and (10) are solved with a Runge-Kutta method of order 8 with step-size control [31,32]. The time step size is about $0.01fs$, and the "global time step" has been set as $1fs$. In most of this work, we take a polyacene chain composed of $m = 100$ aromatic rings, which is long enough in the cases considered. The other parameters are those generally chosen for polyacene [19–23]: $t_0 = 2.5$ eV, $\alpha = 4.1$ eV/Å, $K = 15.5$ eV/Å^2, $M = 1349.14$ eV fs^2/Å^2, and $2t_1 = 0.864t_0$. A small damping is also introduced to smear out the lattice vibrations so that the localized lattice distortions can be seen clearly.

Additionally, to identify the formation and evolution of the localized electronic states, we define the degree of localization, $\gamma_i = \sum_{j,n}|\varphi_{j,n,i}(t)|^4 / \sum_{j,n}|\varphi_{j,n,i}(t)|^2$, for electronic state i, here $\varphi_{j,n,i}$ is the electronic eigenfunction at the nth site of the jth chain. It will decay as $1/m$ for an extended state when the size m becomes larger and larger, while it approach a nonzero constant for a localized state. We have done calculations for various chain length, and a very good convergence for γ_i is reached for a polyacene chain composed of $m = 100$ aromatic rings, for which all results presented below are obtained.

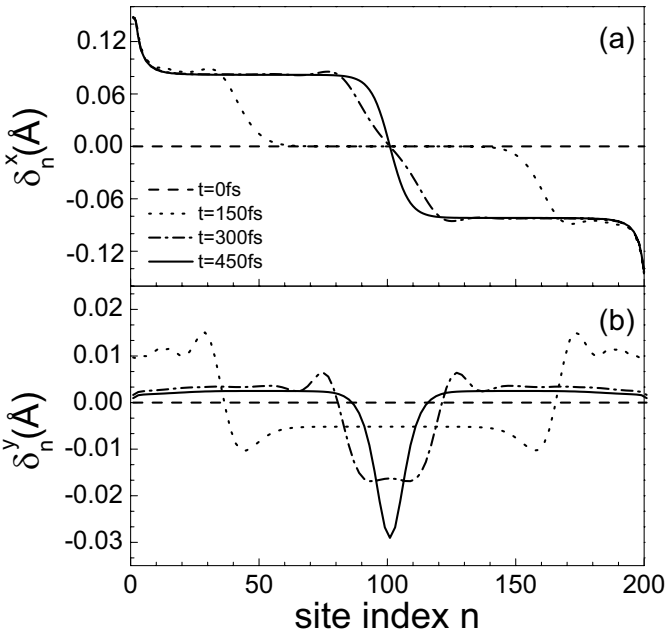

Fig. 2. Formation of an interchain coupled soliton in a pristine polyacene chain. The staggered bond parameters δ^x_n (a) and δ^y_n (b) at various times are shown.

3 Results and discussions

3.1 Initial configuration

First of all, we discuss the bond structure and energy spectrum of the ground state of a pristine polyacene chain, which will be taken as the initial configuration of calculations discussed in Sections 3.2 and 3.3. Starting from an undimerized chain, $u^x_n, u^y_n = 0$, we have calculated the evolution of both the bond configuration and the electronic states to seek the stable state with minimum energy. Figure 2 shows the staggered bond parameters, $\delta^x_n \equiv (-1)^n\left(u^x_{j,n+1} - u^x_{j,n}\right)$ (only the bond parameters of chain 1 are plotted, because they are identical with those of chain 2) and $\delta^y_n \equiv u^y_{1,n} - u^y_{2,n}$, at different times. One can find that the undimerized lattice structure is not stable. In chain direction (δ^x_n), the kinks appear firstly at the chain ends, then they move toward to the middle of the chain, at last, they combine to form a soliton-like distortion in the chain, which should be a consequence of odd-number sites in each chain. After 400 fs, the bond parameters tend to stable. The stable bond structure is consistent with that obtained by solving self-consistent electron-lattice coupling equations (4), (5) and (6) [22]. Moreover, accompanying the lattice distortion in chain direction, the bond-lengths are changed for those bonds

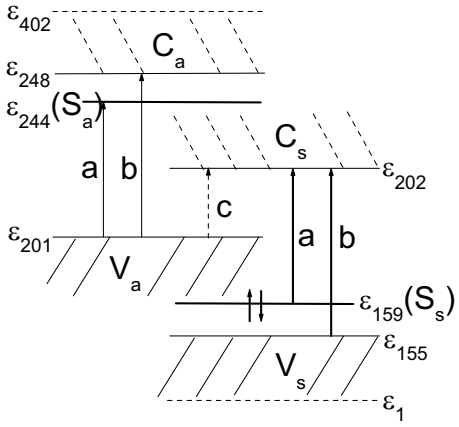

Fig. 3. Schematic representation of the energy spectrum of a neutral pristine polyacene chain. The solid lines with arrows indicate the dipole-allowed transitions for light polarized parallel to the chain, and the dashed lines with arrows indicate the dipole-allowed transitions for light polarized perpendicular to the chain.

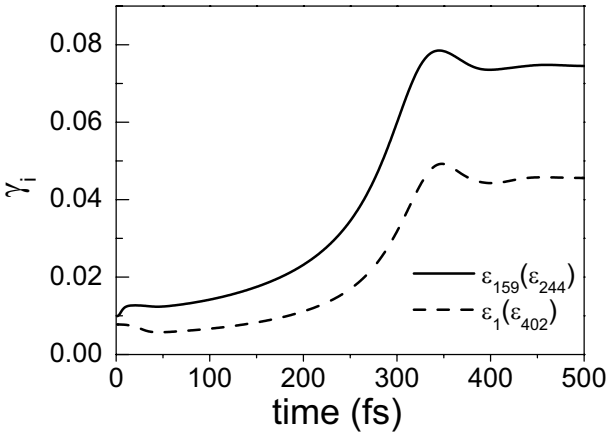

Fig. 4. The degrees of localization of eigenstates vary with time for a pristine polyacene chain.

linking the two chains (δ_n^y), although the amplitude is smaller than that in chain direction. It should be stressed that the bonds linking the two chains become shorter near the soliton kink in the chain. Ab initio calculations on short polyacene chains have shown that the cross bonds in the middle of chain are slightly shorter than those at chain ends [33], so our result is consistent with that of ab initio calculations. The two soliton-like distortions in the two chains are not free each other but bound closely due to the strong interchain coupling, therefore, the shorter cross bonds could strengthen the coupling between them. We should also note that the interchain coupled soliton is a neutral singlet, against the spin-charge relation of solitons in a single polyacetylene (neutral with spin 1/2 or charged with spin 0).

The schematic representation of energy spectrum of a neutral pristine polyacene is plotted in Figure 3. Four energy bands have been identified, moreover, the two down-shift branches (denoted by "s") have symmetric wave functions for the two chains in polyacene and the two up-shift

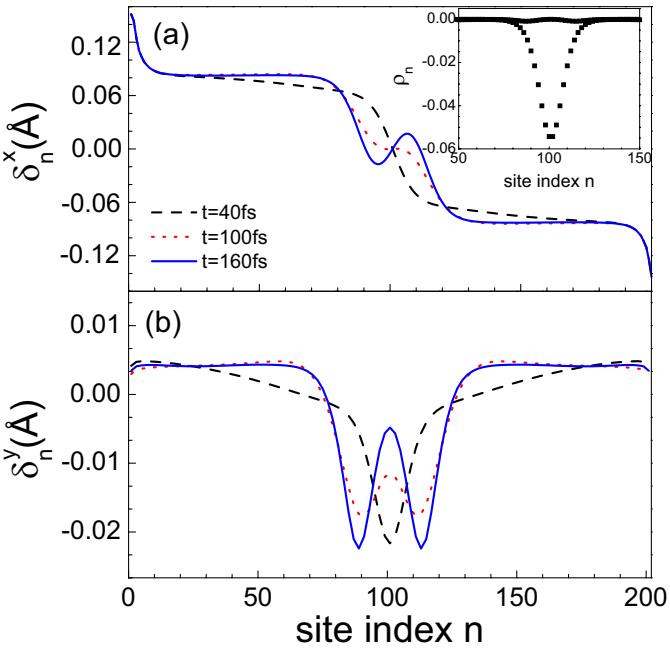

Fig. 5. Formation of a polaron-like distortion in a charged polyacene chain. The staggered bond parameters δ_n^x (a) and δ_n^y (b) at various times are shown. The inset shows the charge density distribution along the chain at $t = 160$ fs.

ones (denoted by "a") have antisymmetric wave functions. Furthermore, along with the localized lattice deformation, there appear two localized electronic states $S_a(\varepsilon_{244})$ and $S_s(\varepsilon_{159})$. However, in contrast to that in a single polyacetylene chain where the localized soliton states are in the midgap, these two localized states are split due to the strong interchain coupling so that one (S_a) goes up with the up-shift conduction band (C_a) and the other one (S_s) goes down with the down-shift valence band (V_s). Besides the soliton energy levels, there are other two localized states, one at the bottom of valence band (ε_1) and another at the top of conduction band (ε_{402}). This is similar as the case of trans-polyacetylene [34]. The formation and evolution of these localized electronic states could be seen easily through the variation of their degree of localization, γ_i, as shown in Figure 4. We can find that the formation of these localized states as well as the interchain coupled soliton is at around $t = 400$ fs.

3.2 Dynamics of excitation induced by charge injection

Now, taking the lattice configuration at the ground state of a pristine polyacene obtained in the above section, we investigate the dynamics after the injection of an electron (or a hole), e.g., by doping or injection from the electrode. For that, we add one extra electron into the lowest unoccupied molecular orbital (LUMO) at time zero. In this case, the lattice is not stable any longer, it will relax toward the lower energy state. Figure 5 illustrates how the electron self-consistently distorts the lattice and is localized in the deformation (Only the bond parameters in chain 1

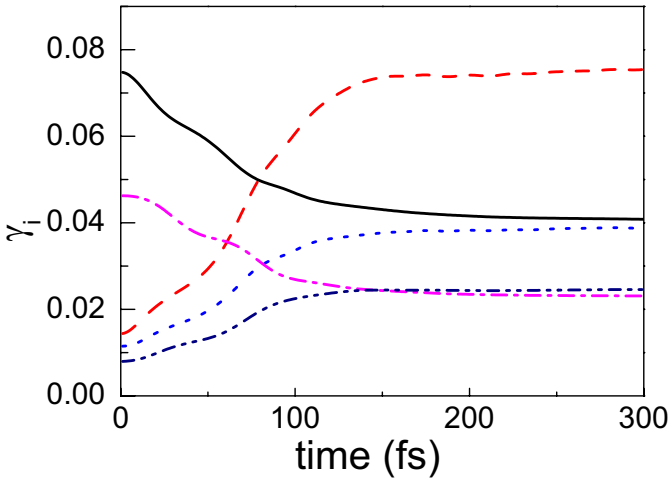

Fig. 6. The degrees of localization of eigenstates vary with time for a singly charged polyacene chain. Solid line for ε_{159} (ε_{244}); dash line for ε_{201} (ε_{202}); dot line for ε_{156} (ε_{247}); dash-dot line for ε_1 (ε_{402}); dash-dot-dot line for ε_2 (ε_{401}).

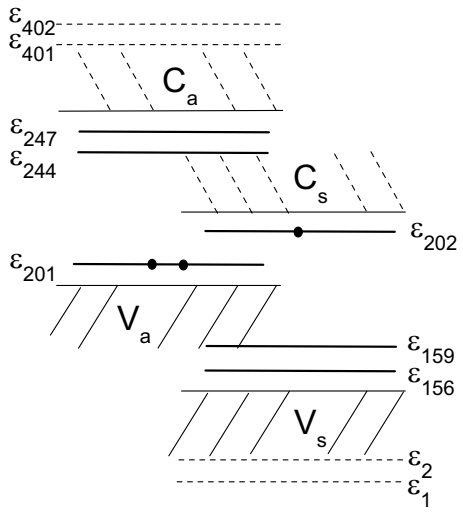

Fig. 7. Schematic representation of the energy spectrum of a singly charged polyacene chain.

are plotted, which is identical to those in chain 2). In the chain direction, as time progresses, the width of the soliton increases gradually, then a polaron-like distortion in the center of the soliton is formed at about 150 fs. At the same time, in the direction vertical to the chain, the distortion of cross bonds becomes wider with the width of soliton stretched. Finally, one can find that the cross bonds corresponding to the polaron part are longer than those to the neutral soliton part. This could indicate that the coupling between the polarons is weaker than that of solitons. It should be stressed that the extra electron is localized in the middle polaron region of the chain, as shown in the inset of Figure 5, which indicates the interchain polaron is one of the charge carriers in polyacene chain. Another dynamical characteristic is that, in contrast to the single polyacetylene case [25], there is less lattice vibration appearing in the relaxation. This can be understood as that less electronic energy has been transferred into the lattice in the process due to the smaller band gap. However, a similar vibrational behavior of polaron amplitude has been found [35].

For a singly charged polyacene chain, ten localized electronic states are found, their variations of localization-degree with time are shown in Figure 6. Among them, two (ε_{159} and ε_{244}) are the soliton levels similar as those in a neutral pristine polyacene, however, their degrees of localization decrease comparing with those in neutral case; Along with the formation of interchain polaron, four extended electronic states become localized ones (two (ε_{201} and ε_{202}) appear in the gap while the other two (ε_{156} and ε_{247}) are located near the bottom of C_a and the top of V_s, respectively); For the four localized levels located at the top of conduction band and the bottom of the valence band, respectively, two (ε_1 and ε_{402}) have been found in the neutral case, only their localization-degrees decrease, the other two (ε_2 and ε_{401}) emerge when the coupled polaron is formed. The schematic representation of energy spectrum of a singly charged polyacene and the positions of localized electronic states are plotted in Figure 7.

3.3 Dynamics of photoexcitations

Another way to excite a polymer to generate elementary excitations is through photoexcitation. In a previous work [22], we have discussed the absorption spectrum of the ground state of polyacene chain, i.e., the neutral pristine polyacene chain, and three main absorption characteristics have been found. According to the symmetries of wave functions for the two chains in polyacene, one can find that the transitions between the bands with the same symmetry, i.e. $V_a \rightarrow C_a$ and $V_s \rightarrow C_s$, are dipole-allowed for light polarized parallel to the chain, while the transitions between bands with different symmetries, e.g., $V_a \rightarrow C_s$, are dipole-forbidden, on the other hand, for light polarized perpendicular to the chain, the dipole selection rule is just reversed. As shown in Figure 3, there are two main features for light polarized parallel to the chain, one arises from the soliton levels (solid line (a)), another is the continuous absorption edge arises from the transition of $V_a \rightarrow C_a$ and $V_s \rightarrow C_s$ (solid line (b)). For the light polarized perpendicular to the chain, the lowest energy absorption is the continuous absorption edge arises from the transition of $V_a \rightarrow C_s$ (dash line (c)). Following these absorption features, we will investigate the lattice dynamic relaxation of photoexcitation states for the following three cases.

3.3.1 Electron transition from HOMO to the soliton level

When one electron is excited from the valence band edge state $\varepsilon_n (n = 201$ in our case) to the soliton level $S_a(\varepsilon_{244})$ (a symmetric case is $S_s(\varepsilon_{159}) \rightarrow \varepsilon_{202}$), an electron-hole pair is created. The electron in the soliton level is relatively stable, and will not induce further lattice distortion, which

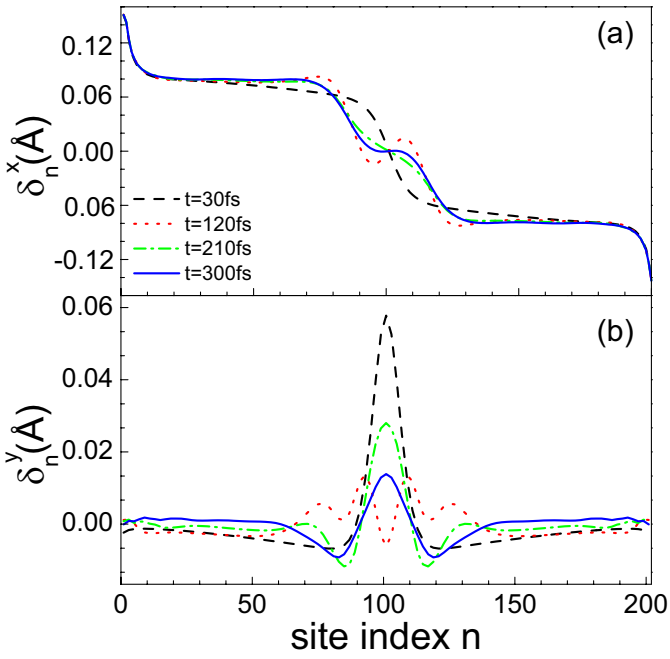

Fig. 8. The staggered bond parameters δ_n^x (a) and δ_n^y (b) for the case that one electron is excited from HOMO to the soliton level.

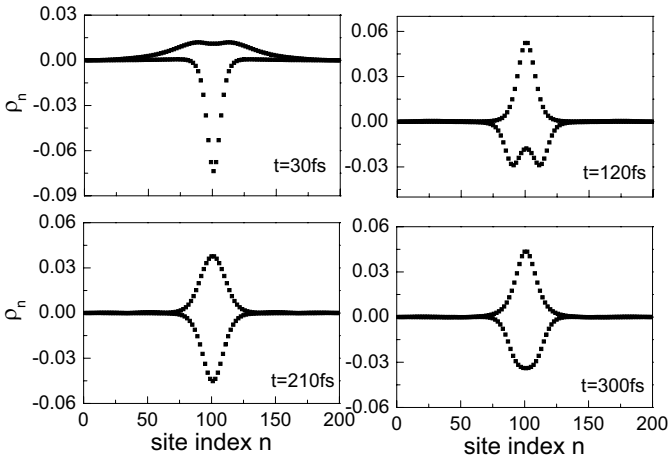

Fig. 9. The charge density distribution in chain for the case that one electron is excited from HOMO to the soliton level.

is similar as that in polyacetylene, where only the neutral soliton becomes charged one. However, the hole left in ε_{201} is not stable, and will result in lattice relaxation, at last, a polaron-like deformation is formed. As expected, this lattice relaxation process should be very similar as that for one electron injection. Figure 8 shows the staggered bond parameters, δ_n^x and δ_n^y, at various times. Comparing Figures 5 and 8, one can find that the amplitude of the polaron distortion is smaller than that in charge injection case, moreover, it shows a larger vibration of polaron amplitude. At the same time, δ_n^y also shows a different feature. This maybe arises from the different occupation of electrons on the eigenstates.

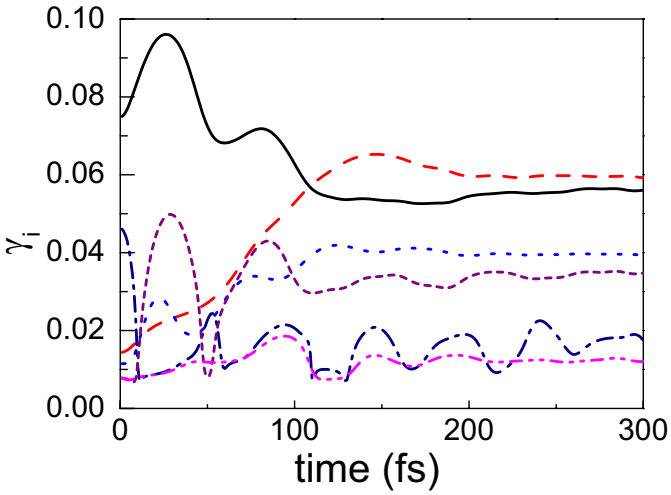

Fig. 10. The degrees of localization of eigenstates vary with time for the case that one electron is excited from HOMO to the soliton level. Solid line for ε_{159} (ε_{244}); dash line for ε_{201} (ε_{202}); dot line for ε_{156} (ε_{247}); dash-dot line for ε_1 (ε_{402}); dash-dot-dot line for ε_2 (ε_{401}); short dash line for ε_{65} (ε_{338}).

The evolution of charge distribution is shown in Figure 9. Initially, the electron is localized in the soliton level and the hole is located in the extended state. Then, the polaron-like distortion is formed at around 120 fs, and the extended state becomes localized one. At the same time, the soliton is stretched, the electron localized in the soliton region shifts away from the center of chain. It is very interesting that the centers of the electron and the hole are separated. This indicates that they could be easily separated by external electric field to become free charge carriers in this process, because the interaction between the soliton and the polaron is weak. Similarly, Köhler et al. has found the electron and the hole are spatially separated in some higher-lying excited states of poly(p-phenylene vinylene)s (PPVs), and the charge separation is facilitated in these states [36]. However, this structure is not the most stable, after several tens of femtoseconds, both δ_n^x and δ_n^y modulate slightly, and it shows an oscillation of the width and depth of polaron. Accompanying the oscillation, the charge density distribution varies with time.

In this case, twelve localized electronic states are found, their variations of localization-degree with time are shown in Figure 10. Besides ten of which have been found in a singly charged chain, see Figures 6 and 7, there are two new localized states (ε_{65} and ε_{338}) located at the bottom of V_a and the top of C_S, respectively. Comparing Figures 6 and 10, one can find that the localization-degrees of polaron energy levels (ε_{201} and ε_{202}) are smaller than those in singly charged polyacene chain, but the degrees of localization of the soliton levels (ε_{159} and ε_{244}) are larger than those in a singly charged polyacene chain. This also implies that the amplitude of polaron distortion in this case is smaller than that in a singly charged polyacene chain, as shown in the evolution of bond parameters, Figures 5 and 8. Furthermore, the localization-degrees of the energy levels located at the bottom of the valence band (ε_1 and

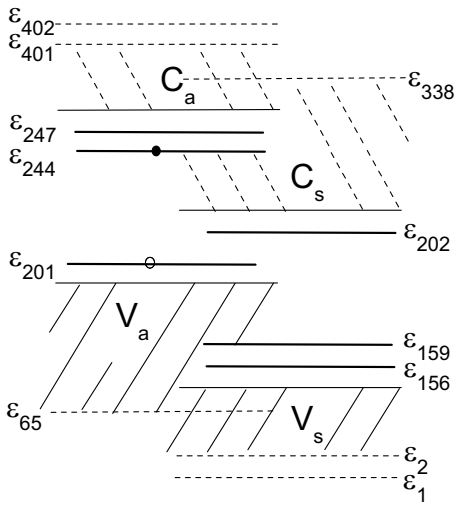

Fig. 11. Schematic representation of the energy spectrum for the case that one electron is excited from HOMO to the soliton level.

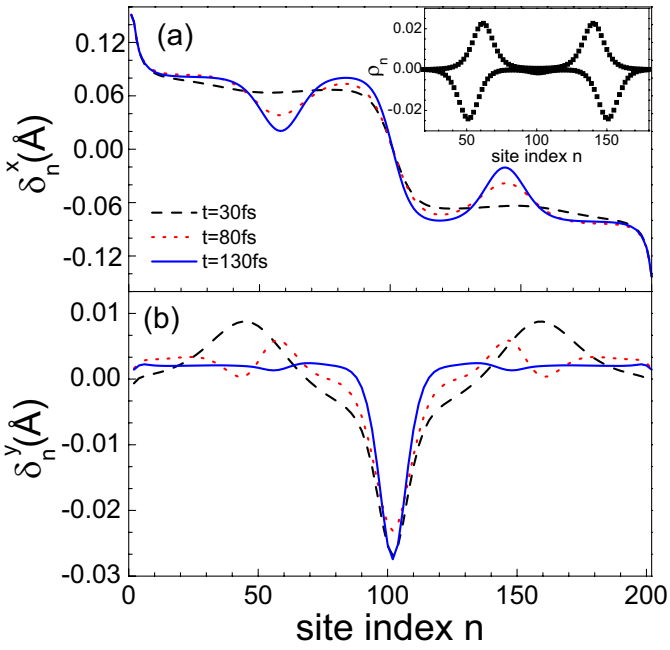

Fig. 12. The staggered bond parameters δ_n^x and δ_n^y for the case of electron-hole pair excited at continuum absorbtion edge for light polarized parallel to the chain. The inset is charge density distribution at $t = 130$ fs.

ε_2) and the top of the conduction band (ε_{401} and ε_{402}) are also smaller than those in a singly charged polyacene chain. The schematic representation of energy spectrum and the positions of localized electronic states are plotted in Figure 11.

3.3.2 Electron-hole pair excited at continuum absorbtion edge for light polarized parallel to the chain

After the polyacene chain absorbs a photon polarized parallel to the chain to create an electron-hole pair between

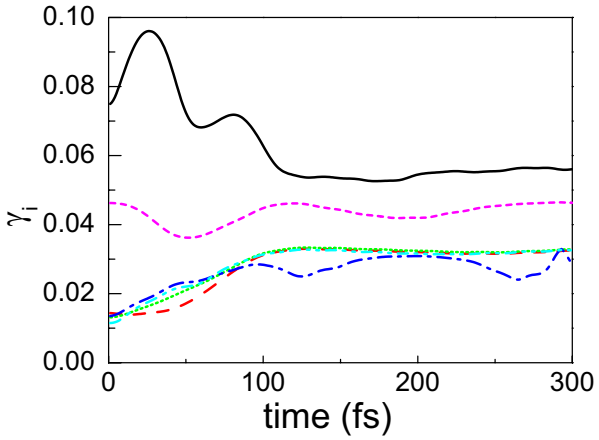

Fig. 13. The degrees of localization of eigenstates vary with time for the case of electron-hole pair excited at continuum absorbtion edge for light polarized parallel to the chain. Solid line for ε_{159} (ε_{244}); dash line for ε_{201} (ε_{202}); dot line for ε_{200} (ε_{203}); dash-dot line for ε_{156} (ε_{247}); dash-dot-dot line for ε_{155} (ε_{248}); short dash line for ε_1 (ε_{402}).

HOMO (ε_{201} in our case) and the conduction band edge state (ε_{248} in our case) (the same as that for $\varepsilon_{155} \rightarrow \varepsilon_{202}$ due to the electron-hole symmetry), the lattice relaxes constantly to form two polaron-like distortions besides the initial neutral soliton, The staggered bond parameters δ_n^x and δ_n^y are shown in Figure 12. The soliton in the center of the chain is still neutral, not affected almost by the excitation, the electron and hole are localized in the two regions of polaron-like distortions. The inset of Figure 12 shows the final charge density distribution. It is the most interesting that the centers of the electron-hole localized in the polarons do not coincide but separate each other about 10 lattice constant. The reason is that the electron localized in the polaron state near C_a distributes on the odd sites, while the hole localized in the gap-polaron state distributes on the even sites. Apparently, this results from the strong interchain coupling, since it has been known that the charge distributes on both even and odd sites in the polaron state for single polyacetylene chain case. As discussed in the case that one electron is excited from HOMO to the soliton level, the electron and hole separation is facilitated in this process.

In this case, twelve localized electronic states are found, their variations of localization-degree with time are shown in Figure 13. Among them, two (ε_{159} and ε_{244}) are corresponding to the soliton levels similar as those in a neutral pristine polyacene, but, their localization-degrees decrease further; Along with the formation of the two polaron-like deformations, eight extended electronic states become localized ones (four (ε_{200}, ε_{201}, ε_{202} and ε_{203}) appear in the gap while the other four (ε_{155} and ε_{156}, ε_{247} and ε_{248}) are located near the bottom of C_a and the top of V_s, respectively); The other two localized levels are located at the top of conduction band (ε_{401}) and the bottom valence band (ε_1), which have been found in the pristine polyacene case. The schematic representation of energy

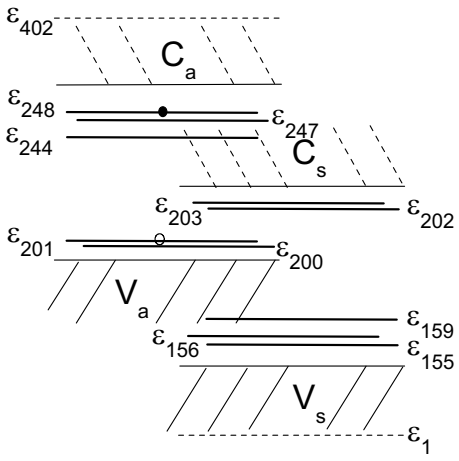

Fig. 14. Schematic representation of the energy spectrum for the case of electron-hole pair excited at continuum absorbtion edge for light polarized parallel to the chain.

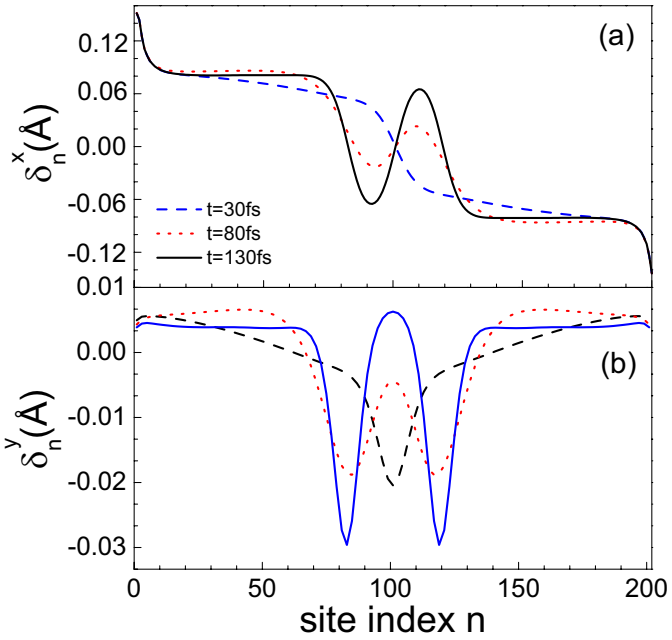

Fig. 15. The staggered bond parameters δ_n^x and δ_n^y versus the sites for the case that one electron is excited from HOMO to LUMO for light polarized perpendicular to the chain.

spectrum and the positions of localized electronic states are plotted in Figure 14.

3.3.3 Electron transition from HOMO to LUMO

When an electron is excited from valence band edge state ε_{201} (HOMO) to the conduction band edge state ε_{202} (LUMO) by light polarized perpendicular to the chain, the electron-hole pair distorts the lattice continuously and is trapped self-consistently in the distortion. At last, in the chain direction, three solitons are obtained, see Figure 15a; vertical to the chain, there are two deformations at positions corresponding to the solitons at left and right hands, see Figure 15b. For the charge distribution, in contrast to the cases of light polarized parallel to the chain,

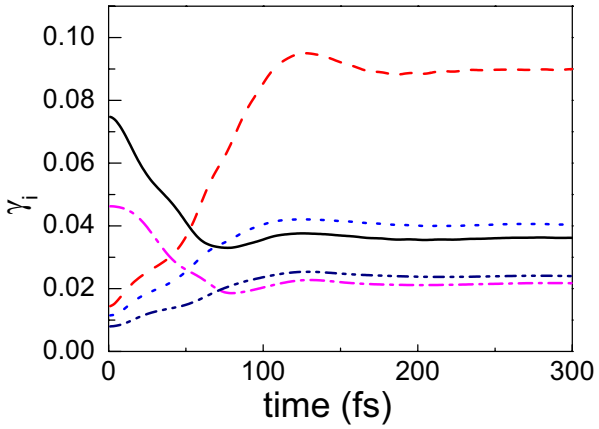

Fig. 16. The degrees of localization of eigenstates vary with time for the case that one electron is excited from HOMO to LUMO for light polarized perpendicular to the chain. Solid line for ε_{159} (ε_{244}); dash line for ε_{201} (ε_{202}); dot line for ε_{156} (ε_{247}); dash-dot line for ε_1 (ε_{402}); dash-dot-dot line for ε_2 (ε_{401}).

where the electron and hole are located at different sites, it shows neutral in the whole chain, which indicates the electron-hole coincides perfectly.

Correspondingly, ten localized electronic states are found, their variations of localization-degree with time are depicted in Figure 16, furthermore, their positions in the energy spectrum are shown in Figure 17. In the gap, the two degenerate localized levels (ε_{201} and ε_{202}) are attributed to the middle soliton according to their wave functions, and they show the most localized characteristic. The degeneration implies that there is no interchain interactions between the middle soliton pair, this feature could also be seen in the variation of δ_n^y, Figure 15b. Additionally, the electron and hole are located on the two localized states, so the electron-hole pair is localized in the middle soliton. Four localized levels located in the valence band (ε_{156} and ε_{159}) and conduction band (ε_{244} and ε_{247}) are attributed to the two interchain solitons at the left and right hands, similar as the case of the neutral pristine chain, they are split due to the strong interchain coupling. Moreover, they are neutral because ε_{156} and ε_{159} are double occupation, and ε_{244} and ε_{247} are vacancy, which are the same with that found in pristine polyacene chain. The other four localized levels are located at the top of conduction band (ε_{401} and ε_{402}) and the bottom valence band (ε_1 and ε_2), respectively.

4 Summary

In summary, using a lattice dynamic model, we have investigated the dynamic formation of elementary excitations induced by both charge injection and photoexcitations in a polyacene chain. Their formation time is found to be about hundred of femtoseconds. Different characteristics of lattice distortions have been identified for various kinds of excitations. Due to the strong interchain interactions, both lattice deformations and the properties of electronic states are remarkably different from those in single polyacetylene chain. Especially, the centers of electron and the

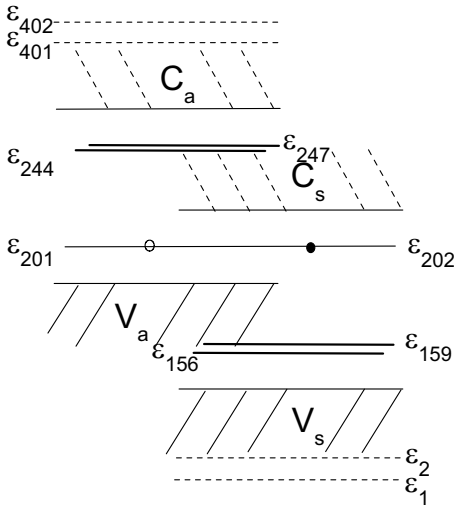

Fig. 17. Schematic representation of the energy spectrum for the case that one electron is excited from HOMO to LUMO for light polarized perpendicular to the chain.

hole in the excited states, which are created by light polarized parallel to the chain, are separated, thus it should be expected that the charge separation is facilitated in polyacene.

In the end of the present work, we would like to discuss the effect of the Coulomb interaction between electrons, which is not take into account in this work. The reasons are followed. On one side, the role of the electronic correlations in polymers remains controversial [1]. The exciton model, where the electron-electron interaction is dominant, and the band model, where the electron-phonon interaction is dominant, compete each other in the understanding of experimental observations. Recently, the band model has been suggested by the experimental observations of photogenerated directly charge carriers [37–39] and the theoretical investigation of photoexcitations based on a tight-binding electron-phonon interacting model [40]. Thus, it is expected that our results should be valid in the system of a weak electron-electron interactions. On the other side, it is really a challenge to study the dynamics of a many-electron interaction system. We leave it in the future.

The work was supported by National Natural Science Foundation of China (Nos. 10204005, 90403110, 10374017, and 10321003) and the State Ministry of Education of China (No. 20020246006).

References

1. *Primary Photoexcitations in Conjugated Polymers: Molecular Exciton versus Semiconductor Band Model*, edited by N.S. Sariciftci (World Scientific, Singapore, 1997), and references therein
2. F. Garnier, R. Hajlaoui, A. Yassar, P. Srivastava, Science **265**, 1684 (1994)
3. J.H. Burroughes, D.D.C. Bradley, A.R. Brown, R.N. Marks, K. Mackay, R.H. Friend, P.L. Burns, A.B. Holmes, Nature **347**, 539 (1990)
4. J.J.M. Halls, C.A. Walsh, N.C. Greenham, E.A. Marseglia, R.H. Friend, S.C. Moratti, A.B. Holmes, Nature **376**, 498 (1995)
5. G. Yu, J. Gao, J.C. Hummelen, F. Wudl, A.J. Heeger, Science **270**, 1789 (1995)
6. N. Tessler, G.J. Denton, R.H. Friend, Nature **382**, 695 (1996)
7. A.J. Heeger, S. Kivelson, J.R. Schrieffer, W.P. Su, Rev. Mod. Phys. **60**, 781 (1988)
8. D. Baeriswyl, K. Maki, Phys. Rev. B **38**, 8135 (1988)
9. J.A. Blackman, M.K. Sabra, Phys. Rev. B **47**, 15437 (1993)
10. Z.J. Li, Z. An, K.L. Yao, Z. Phys. B **97**, 499 (1995)
11. L. Salem, H.C. Longuet-Higgins, Proc. R. Soc. London, Ser. A **255**, 435 (1960)
12. S. Kivelson, O.L. Chapman, Phys. Rev. B **28**, 7236 (1983)
13. M.H. Whangbo, R. Hoffman, R.B. Woodward, Proc. R. Soc. London, Ser. A **366**, 23 (1979)
14. K. Tanaka, K. Ozheki, S. Nankai, T. Yamabe, H. Shirakawa, J. Phys. Chem. Solids **44**, 1069 (1983)
15. A.L.S. da Rosa, C.P. de Melo, Phys. Rev. B **38**, 5430 (1988)
16. B. Srinivasan, S. Ramasesha, Phys. Rev. B **57**, 8927 (1998)
17. C. Raghu, Y.A. Pati, S. Ramasesha, Phys. Rev. B **65**, 155204 (2002)
18. I. Božović, Phys. Rev. B **32**, 8136 (1985)
19. M.K. Sabra, Phys. Rev. B **53**, 1269 (1996)
20. Z.J. Li, H.Q. Lin, K.L. Yao, Z. Phys. B **104**, 77 (1997)
21. Z.J. Li, H.B. Xu, K.L. Yao, Modern Phys. Lett. B **11**, 477 (1997)
22. Z. An, C.Q. Wu, Int. J. Modern Phys. B **17**, 2023 (2003)
23. Y.J. Wu, H. Zhao, Z. An, C.Q. Wu, J. Phys.: Condens. Matter **14**, L341 (2002)
24. W.P. Su, J.R. Schrieffer, A.J. Heeger, Phys. Rev. Lett. **42**, 1698 (1979); W.P. Su, J.R. Schrieffer, A.J. Heeger, Phys. Rev. B **22**, 2099 (1980)
25. W.P. Su, J.R. Schrieffer, Proc. Natl. Acad. Sci. USA **77**, 5626 (1980)
26. E.J. Mele, Phys. Rev. B **26**, 6901 (1982)
27. C.Q. Wu, Y. Qiu, Z. An, K. Nasu, Phys. Rev. B **68**, 125416 (2003)
28. Å. Johansson, S. Stafström, Phys. Rev. Lett. **86**, 3602 (2001)
29. S. Stafström, K.A. Chao, Phys. Rev. B **30**, 2098 (1984)
30. Z. An, Z.J. Li, Y. Liu, Y.C. Li, Chinese Phys. **9**, 37 (2000)
31. R.W. Brankin, I. Gladwell, L.F. Shampine, RKSUITE: Software for ODE IVPS (`www.netlib.org`)
32. H.W. Streitwolf, Phys. Rev. B **58**, 14356 (1998)
33. Z. An, C.Q. Wu (unpublished)
34. R. Fu, S. Xie, C.Q. Wu, X. Sun, Chin. Phys. Lett. **4**, 349 (1987)
35. H. Zhao, Z. An, C.Q. Wu, to be published in Eur. Phys. J. B
36. A. Köhler, D.A. dos Santos, D. Beljonne, Z. Shuai, J.L. Bredas, A.B. Holmes, A. Kraus, K. Mullen, R.H. Friend, Nature **392**, 903 (1998)
37. P.B. Miranda et al., Phys. Rev. B **64**, 81201 (2001)
38. D. Moses, A. Dogariu, A.J. Heeger, Chem. Phys. Lett. **316**, 356 (2000); D. Moses, A. Dogariu, A.J. Heeger, Phys. Rev. B **61**, 9373 (2000); D. Moses, A. Dogariu, A.J. Heeger, Synth. Met. **116**, 19 (2001)
39. P.B. Miranda et al., Synth. Met. **119**, 619 (2001)
40. Z. An, C.Q. Wu, X. Sun, Phys. Rev. Lett. **93**, 216407 (2004)